Carbohydrate Polymers 109 (2014) 92–101

Contents lists available at ScienceDirect

Carbohydrate Polymers

journal homepage: www.elsevier.com/locate/carbpol

Chitosan-glutaraldehyde copolymers and their sorption properties

Louis Poon [a], Lee D. Wilson [a,*], John V. Headley [b]

[a] Department of Chemistry, University of Saskatchewan, 110 Science Place, Saskatoon, Saskatchewan S7N 5C9, Canada
[b] Aquatic Contaminants Research Division, Water Science and Technology Directorate, 11 Innovation Boulevard, Saskatoon, Saskatchewan S7N 3H5, Canada

ARTICLE INFO

Article history:
Received 5 September 2013
Received in revised form 26 February 2014
Accepted 28 February 2014
Available online 13 March 2014

Keywords:
p-Nitrophenol
Adsorption
Isotherm
Chitosan
Glutaraldehyde
Copolymer

ABSTRACT

This study reports the preparation of chitosan-glutaraldehyde (Chi-Glu) copolymers at modified reaction conditions such as the temperature prior to gelation, pH, and reagent ratios. The chitosan copolymers were characterized using infrared spectroscopy (FT-IR), CHN elemental analysis, and thermal gravimetric analysis (TGA). Evidence of self-polymerized glutaraldehyde was supported by CHN and TGA results. The sorption properties of Chi-Glu copolymers were evaluated in aqueous solutions containing *p*-nitrophenol at variable pH (4.6, 6.6, and 9.0). The sorption properties of the copolymers correlated with the level of the accessibility of the sorption sites in accordance with the relative cross-linker content. The relative sorption capacity of the Chi-Glu copolymers increases as the level of cross-linking increases. Chitosan displays the lowest sorptive uptake while an optimal sorption capacity was concluded at the 4:1 glutaraldehyde:chitosan monomer mole ratio, in close agreement with the three reactive sites (i.e. —OH/—NH) per glucosamine monomer. The PNP dye probe was determined to bind to chitosan through an electrostatic interaction due to the increased sorption capacity of the phenolate anion, as evidenced by the change in pH from 4.6 to 9.0.

1. Introduction

Chitosan was first discovered in 1859 by Rouget when chitin was boiled in concentrated potassium hydroxide and the subsequent product was shown to be soluble in acids (Muzzarelli, 1977). Chitosan is rarely found in nature but can be obtained from hydrolysis of chitin. Each year, approximately 20 million tonnes of shrimp, lobster, and crab shells are discarded as waste by-products (Bruck, Slater, & Carney, 2010). Thus, synthetically engineered chitosan copolymers represent a versatile biomaterial platform for wastewater treatment applications because of its relative availability and amenability to chemical modification. Chitosan is a polysaccharide containing two types of monomer: 2-acetamido-2-deoxy-D-glucopyranose and 2-amino-2-deoxy-β-D-glucopyranose. The pK_a of chitosan ranges between 5.5 and 6.5 depending on the degree of deacetylation and its average molecular weight may cover a range of possible values (e.g., 1–5 × 10^5 g/mol).

Due to the semi-crystalline nature of chitosan and its relatively low surface area (Piron et al., 1997), it is generally a poor adsorbent of organic dye species in its unmodified form. Therefore, much of the application of chitosan copolymers employs the use of cross-linkers to modify its chemical structure and textural properties by linking at the amine or the hydroxyl sites. Cross-linking between chitosan and glutaraldehyde afford copolymer materials with a porous network with improved adsorption properties (Crini & Badot, 2008). In this manner, chitosan can be structurally modified by forming copolymers with variable morphology (i.e. beads, hydrogels, powders, and films/membranes). Such materials have tunable structure and physicochemical properties as evidenced by their diverse applications; self-repairing materials (Ghosh & Urban, 2009), biopolymer-based membranes for chemical separations (Chen, Zheng, Wang, Lee, & Park, 2002), wastewater and dye remediation (Chiou & Chuang, 2006; Jin & Bai, 2002; Xu, Hein, Loo, & Wang, 2008), and drug delivery systems (Bodnar, Hartmann, & Borbely, 2006; Jafarinejad et al., 2012; Lu et al., 2012; Ma, Qian, Yang, Hu, & Nie, 2010; Shu & Zhu, 2002). Chitosan copolymers derived from cross-linking with glutaraldehyde (Chi-Glu) were applied in dye remediation since adsorption occurs mainly through the deacetylated sites (i.e. primary amine groups). Ion-dipole and H-bonding are considered the primary noncovalent interactions for the adsorption of dyes (Chiou & Li, 2003; Ngah & Fatinathan, 2006; Pratt, Wilson, & Kozinski, 2013).

Chitosan copolymers are typically prepared using a conventional sol–gel process where chitosan is dissolved in dilute acid to form an aqueous solution where the cross-linkers are subsequently incorporated. To obtain beads, the mixture may be added

* Corresponding author. Tel.: +1 306 966 2961; fax: +1 306 966 4730.
E-mail address: lee.wilson@usask.ca (L.D. Wilson).

http://dx.doi.org/10.1016/j.carbpol.2014.02.086
0144-8617/

drop-wise into an alkali solution where the protonated amine groups are neutralized and subsequently precipitated. Precipitation generally occurs rapidly where the resulting beads have uniform diameters (Jin & Bai, 2002). For conventional copolymers, the viscosity of the chitosan solution with the cross-linker increases with time until the gel point is reached; thereafter, the cross-linked chitosan solution forms a gel phase. Gelation depends on various factors but can be accelerated by increasing the pH along with mechanical mixing so that the solution approaches the pK_a of chitosan (Kildeeva, Perminov, Vladimirov, Novikov, & Mikhailov, 2009). An ageing process of the gel sets in where the shear modulus increases with eventual hardening (Kildeeva et al., 2009). An insoluble cross-linked copolymer is obtained once the gel network is dehydrated and neutralized by adding additional alkali solution to precipitate out the copolymer followed by air drying.

The relationship between the gelation process and the degree of cross-linking is poorly understood. The ageing process is known to affect the porosity of the xerogel that forms after drying (Brinker & Scherer, 1990), and ageing may occur over days depending on the type of gel because the overall structure may drastically change (Brinker & Scherer, 1990). For example; the average pore width of titania gel systems (Brinker & Scherer, 1990) increases from 3 to 7 nm after ageing for one day. The dependence of the size of the pores with ageing of the gel likely affects the surface accessibility of the pores and the overall sorption capacity (Brinker & Scherer, 1990; Kyzas et al., 2010). As well, the influence of pH on the morphological properties of gels is anticipated since an increase in the shear modulus of the gel was noted elsewhere (Kildeeva et al., 2009) as the pH increased from 4.1 to 5.6 for a chitosan-glutaraldehyde solution. The textural and chemical properties of the copolymer are related to the overall sorption capacity of the final product.

Therefore, the objective of this paper was to investigate the effect of pH, temperature, and cross-linker content on the sorption capacity of chitosan cross-linked with glutaraldehyde (Chi-Glu). Herein, we describe the synthesis, characterization, and equilibrium sorption properties of aged Chi-Glu copolymers with *p*-nitrophenol (PNP) in aqueous solutions. Dyes such as PNP have been shown to serve as reliable adsorptive probes for studying the physicochemical properties of copolymers in heterogeneous systems at different experimental conditions (Mansri, Memou, & Benabadji, 2013; Wilson, Mohamed, & Headley, 2011).

2. Experimental

2.1. Materials

Sodium hydroxide, potassium phosphate monobasic, *p*-nitrophenol, low molecular weight chitosan (75–85% deacetylated, molecular weight range: 50,000–190,000 kDa), 50%(w/w) glutaraldehyde in water, and glacial acetic acid were obtained from Sigma–Aldrich Canada Ltd. (Oakville, ON). Granular Activated Carbon (GAC; Norit Rox 0.8) was obtained from Norit America and used as received after drying under vacuum. All other chemicals were used as received unless specified otherwise.

2.2. Synthesis of chitosan cross-linked glutaraldehyde copolymers

6.00 g of chitosan (50,000–190,000 g/mol) was dissolved in 600 mL of aqueous acetic acid (5%, v/v). Upon dissolution, glutaraldehyde was diluted with an additional 20 mL (5%, v/v) aqueous acetic acid (pH = 3.3–3.9) and added to the chitosan solution. The amount of glutaraldehyde added was related to the relative mole ratio of chitosan monomer, as shown in Table 1. The solution was stirred overnight at 295 K until a light yellow to orange coloured gel was obtained. The removal of excess water (200–300 ml) under vacuum was done with gentle heating at 25–30 °C if gelation did not occur within 24 h. Upon gelation, the mixture was allowed to stand for 24 h to facilitate the ageing process. Upon completion of ageing, a 6 M aqueous sodium hydroxide solution was added slowly over 1 h to the gel with rigorous stirring with a spatula. The gel formed an insoluble brown precipitate and the pH of the supernatant solution was maintained at 7.0. The suspension was left in the solution overnight and a dark brown product was obtained and was isolated with vacuum filtration. A dark brown hydrogel was obtained and broken into smaller pieces with a spatula and ground gently with a mortar and pestle. Gentle drying of the product was carried out for 1 h at 333 K at ambient pressure. The product was periodically removed during the drying process and ground with the mortar and pestle to a fine powder. This procedure of periodic heating and grinding is used to prevent densification of the gel and was repeated until the final product appeared as a fine brown powder which was finally dried for 12 h at 25–30 °C. The final copolymer was then passed through a 40-mesh sieve, followed by washing in a Soxhlet extractor with methanol for 24 h. Finally, a vacuum oven at a temperature of 45 °C and reduced pressure (25 mmHg) was used to remove residual solvents from the copolymer product.

Table 1
Relative amounts of chitosan glutaraldehyde used for the copolymer synthesis. A theoretical mole ratio of glutaraldehyde to number of amine groups of chitosan ratio (Glu/NH_2) is also listed here.

Copolymer product	Mass of chitosan (g)	Volume of glutaraldehyde[a] solution (ml)	Calculated Glu/NH_2 mole ratio[b]
CG-1	6.00	3.6	0.670
CG-2	6.00	6.3	1.17
CG-3	6.00	9.0	1.68

[a] Density of glutaraldehyde solution 50% (w/v) is 1.106 g/L.
[b] Degree of deacetylation (75–85% deacetylated) was accounted for in Table 1. An average of 80% deacetylation was used.

2.3. Copolymer characterization

2.3.1. FT-IR

Fourier Transform IR spectra were obtained using a double beam spectrophotometer (Bruker, model Tensor 27). The sample chamber was purged with nitrogen gas and solid samples were analyzed as KBr pellets in transmission mode. In the case of liquid samples, they were analyzed as a liquid film using a NaF cell.

2.3.2. UV–vis

UV–vis absorbance spectra were obtained using a double beam Varian-Cary (Cary 100) spectrophotometer. Residual dye in aqueous solution was obtained using quartz cuvettes. A calibration curve of absorbance vs. dye concentration was made to determine the linear response region of the Beer–Lambert law and the molar absorptivity (ε) of residual (unbound) PNP at equilibrium for various pH and concentration conditions.

2.3.3. TGA

Thermogravimetry analysis (TGA) of samples was obtained with a TA Instruments analyzer (Model Q50). Nitrogen gas was used for cooling and purging of the sample compartment. Samples were analyzed in open aluminium pans over the temperature range between 30 °C and 500 °C at a nominal heating rate of 10 °C.

2.3.4. CHN analyses

Carbon, hydrogen and nitrogen elemental contents were obtained with a Perkin Elmer 2400 CHN Elemental Analyzer. The combustion oven temperature was above 925 °C while the reduction oven had a temperature over 640 °C. The instrument was

Table 2
Values of λ_{max} and molar absorptivity (ε) for PNP at various pH values.

pH of PNP solution	λ_{max} (nm)	ε ($\times 10^5$ L mol^{-1} cm^{-1})
4.6	318	1.02
6.6	325	0.981
	400	2.09
9.0	400	1.86

Note: Since pH 6.6 is close to the pK_a value of PNP (7.15), a significant portion of PNP is deprotonated to form an anion (PNP^-, λ_{max} = 400 nm) and another portion remains as the protonated form (PNP, λ_{max} = 325 nm). Therefore, the initial concentration of the dye (C_o) is the sum of these two contributions according to the Henderson–Hasselbalch equation.

purged using a mixture of pure oxygen and helium gas. The calibration standard was acetanilide. The standard error of the CHN results are within ±5%.

2.3.5. Scanning electron microscopy (SEM)

SEM images of chitosan and its copolymers were obtained with a Hitachi Scanning Electron Microscope (Model TM-3000) using secondary electron irradiation and 15 kV with 100× magnification. The samples were run at ambient conditions in their pristine form without any surface treatment.

2.4. p-Nitrophenol (PNP) adsorption studies

The molar absorptivity (ε) values for *p*-nitrophenol (PNP) was estimated using the Beer–Lambert calibration plot (*cf.* Table 2). Deviations from the Beer–Lambert law occur when [PNP] > 0.18 mM for pH 4.6; therefore, the supernatant solutions from the adsorption studies were analyzed in the linear region and diluted accordingly. In a typical sorption experiment, 20.0 ± 0.2 mg of copolymers were added to vials. A 10 mM stock solution of PNP was prepared in a 10 mM KH_2PO_4 buffer at pH 4.6. 7.00 ml of PNP solution was added to each vial containing sorbent and blank. The samples were mixed for 48 h at 295 K and then the absorbance of the supernatant was measured using UV–vis spectroscopy after settling of insoluble sorbent material by centrifugation, as outlined above. The same procedure was applied at pH 9.00, where a 10 mM $NaHCO_3$ buffer was pH adjusted using 1 M NaOH. At pH 6.6, a 10 mM KH_2PO_4 buffer was pH adjusted using 1 M NaOH.

2.5. Sorption data analysis

The sorption results are reported as the uptake of adsorbate onto the solid adsorbent phase (Q_e),

$$Q_e = \frac{(C_o - C_e) \times V}{m} \quad (1)$$

where C_o and C_e are the initial and equilibrium dye concentration (mM), respectively. V (L) is volume of dye added to each sample vial containing a fixed mass of sorbent (m; gram units).

2.6. Swelling of chitosan and copolymers

The swelling properties of chitosan and the copolymers in water were determined gravimetrically. A clean, lidless, pre-weighed vial was obtained and 40–50 ± 1 mg of adsorbent was added to the sample vial. 6.00 mL of deionized water was added to each vial and the heterogeneous solid/solution system was shaken for 48 h at 160 rpm. The materials were then removed and using a pre-weighed filter paper, the hydrated copolymers were isolated and tamped dry to remove excess water prior to obtaining final sample weights. The filter paper and the vial were air dried for 12 h. Both the filter paper with the copolymer and the vial containing residual adsorbent was weighed after constant weight (~12 h). The difference between the mass of the hydrated copolymer and the dried copolymer is related to the degree of swelling. The relative amount of swelling (S; %) is given by Eq. (2), where the mass of the hydrated polymer (m_s) and the mass of the dry polymer (m_d) are determined directly.

$$S = \frac{(m_s - m_d) \times 100\%}{m_d} \quad (2)$$

2.7. Error analysis

Errors are calculated according to procedures reported elsewhere in the literature (Kwon & Wilson, 2010; Poon, 2013; Poon et al., 2014).

3. Results and discussion

3.1. Synthesis

Syntheses of the Chi-Glu copolymers were adapted from a previous study (Wilson & Xue, 2013). Upon dissolution of chitosan in acetic acid (pH 3.6–3.9), the resulting aqueous solution has a light yellow colour, and this is attributed to trace amounts of residual oxidized astaxanthin (Henry et al., 2000; Youn, No, & Prinyawiwatkul, 2007) (*cf.* Fig. 1). Upon addition of glutaraldehyde to the chitosan solution, the pale yellow solution becomes a darker orange-yellow colour. This is a qualitative indicator of the cross-linking between glutaraldehyde and the amine groups of chitosan. Previous studies suggest that the colour indicates the presence of unsaturated aldol condensation products such as α, β-unsaturated imines and enal products (Kildeeva et al., 2009). After gentle stirring for 24 h, the Chi-Glu solution undergoes gelation and this process depends on the relative concentration of glutaraldehyde. Gelation was more pronounced for CG-2 and slowest for CG-1 (cf. Table 1), in agreement with previous results (Kildeeva et al., 2009).

3.1.1. Effects of temperature on the Chi-Glu solution (CG-2T)

For the CG-1 and the CG-2 copolymers, there was an excess of aqueous acetic acid solution that occasionally prevents the formation of the polymeric network required for gelation due to electrostatic repulsion between chitosan units. One method to remove the solvent is to evaporate through heating (Wilson & Xue, 2013). This method was investigated by preparing a new CG-2 solution which was then heated to 323–333 K and then allowed to cool to afford a gel phase (CG-2T). Ideally, this method would reduce the volume of solvent but increase the gelation time according to the Arrhenius equation (Brinker & Scherer, 1990). The temperature could be reduced afterwards to increase the gelation rate. An increase in temperature does reduce the volume of water and acetic acid, and this had the unintended effect of also accelerating the rate of aldol condensation between glutaraldehyde and chitosan. At elevated temperatures, most of the aldol undergoes elimination to the more hydrophobic enal and α,β-unsaturated imines. This concurs with the intense dark brown colour of these copolymer products. Secondly, dehydration of the alcohols to form the enal adduct which reduces the number of H-bond donor and acceptor sites and suggests that the volume of water loss to undergo gelation increased. Therefore, elevating the temperature exacerbates the problem of solution retention in the copolymer framework.

3.1.2. Gelation of Chi-Glu copolymers

After 24 h, gelation occurs and the copolymer becomes aged (*cf.* Fig. 1B). The capillary pressure in the gel caused by an increase in cross-linking limits the diffusion of the aqueous alkali solution into the gel network. Therefore, mechanical stirring with a spatula

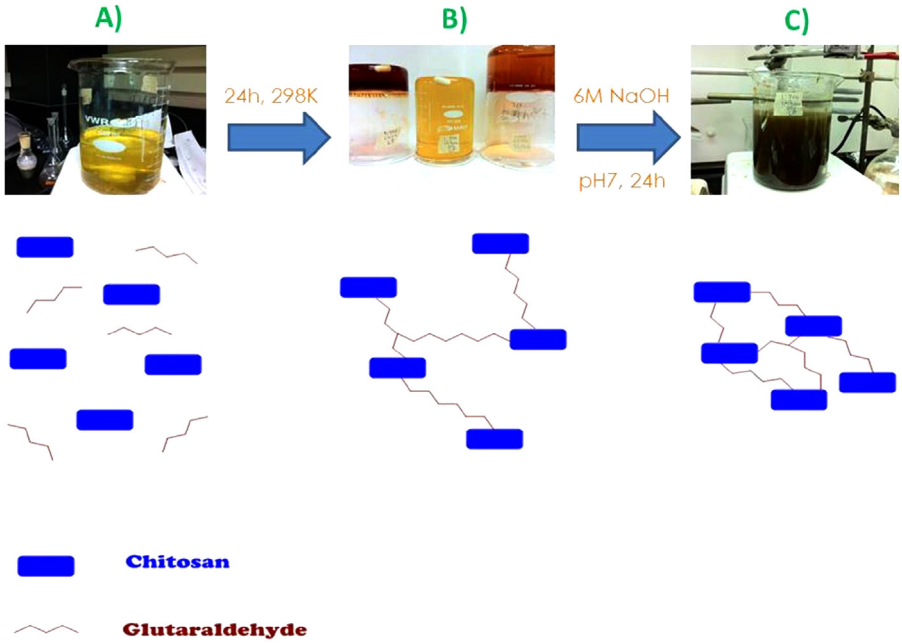

Fig. 1. Sol–gel process for the cross-linking reaction of glutaraldehyde and chitosan in aqueous solution: (A) Chi-Glu Solution, (B) Gelation, and (C) Shrinkage of gel network followed by precipitation. *Note:* The molecular size of chitosan and glutaraldehyde are not drawn to scale.

facilitates exposure of the polymeric network in the gel by contact with the base (NaOH) solution.

3.1.3. *Precipitation of Chi-Glu copolymers*

As more glutaraldehyde is cross-linked with chitosan, the surface of chitosan becomes more hydrophobic and/or less accessible to hydration. As shown in Fig. 2, the transition from (a) to (c) results in phase separation. The darkening of the precipitate indicate that the reaction has gone to completion because the majority of the aldol was converted into the UV-active enal or α,β-unsaturated imine. From these two examples, it can be concluded that polymerization of the glutaraldehyde is continuous and when precipitation of the copolymer occurs it may lower the degree of cross-linking. The physical appearance of the isolated product is noteworthy because CG-3 resembles the texture of the CP-1 material, as described by Wilson and Xue (refer to Fig. 1 by Wilson & Xue, 2013).

3.1.4. *Effect of excess NaOH (CG-1H)*

Adaption of the synthesis protocol reported by Wilson and Xue (2013) afforded precipitates of Chi-Glu copolymers after addition of base to a final pH value ~7. The extent to whether excess NaOH (excess refers to the amount of base used to neutralize the supernatant solution) and its effect on the morphology or the physicochemical properties of Chi-Glu copolymers is of continued interest as applied to the synthesis of chitosan copolymer beads. Alkaline solution results in a densification of the copolymer material. In this study, a CG-1 copolymer was synthesized and isolated where the supernatant solution was pH 12.8, and this product is denoted as CG-1H and compared with CG-1.

3.1.5. *Yield and characteristics of Chi-Glu copolymers*

The product yield was calculated assuming that the glutaraldehyde was cross-linked with chitosan; either through an aldol condensation or an amine-catalyzed aldol addition. Accordingly, such reactions involve the loss of two moles of water for every mole of glutaraldehyde reacted with chitosan (Poon et al., 2014; Poon, 2013). Overall, the yield obtained for the copolymers ranged from 70% to 92%, in agreement with previously reported results (Wilson & Xue, 2013). The reduced yield was attributed to the loss of low molecular weight oligomers of Chi-Glu with greater solubility and/or loss of small particulates during filtration and isolation of copolymer products Table 3.

SEM images were obtained for the copolymers and chitosan (*cf.* Fig. 3). All copolymers were ground using a mortar and pestle followed with sieving to ensure a smaller distribution of particle size. Comparison of the SEM images for CG-1, CG-2, and CG-3 with chitosan reveals slight variation in the morphology among the materials. An observed difference in the particle size for CG-1, CG-2, and CG-3. This coincides with chitosan-based nanoparticles with carboxylic acids described elsewhere (Bodnar, Hartmann, & Borbely, 2005; Bodnar et al., 2006). Effects of densification can be observed for CG-1H where the particle diameter ranges from 1 to 4 mm. In the case of CG-1 particles with a similar cross-linking density have smaller particle size. A similar effect can be seen for CG-2T where the particle size appears larger than CG-2. Overall, the SEM images reveal that the various sorbent materials have limited textural porosity in the dry state, in agreement with nitrogen adsorption results (Poon, 2013).

The copolymer products display a variable brown colour depending on the relative pH conditions and the amount of glutaraldehyde employed (*cf.* Fig. S1). Products with darker colour are observed when the level of glutaraldehyde increases; while all other reaction conditions were held constant. CG-1 displays the

Table 3
Experimental yield of various Chi-Glu copolymers prepared at 298 K and precipitated at pH 7.0 unless stated otherwise.

Copolymers[a]	% Yield[b]
CG-1	81
CG-1H	69
CG-2	87
CG-2T	79
CG-3	83

[a] Copolymers are defined according to the reagent ratios as listed in Table 1.
[b] Yields are calculated according to the reaction in accordance to section 3.1.5. (cf. Poon et al., 2014; Poon, 2013).

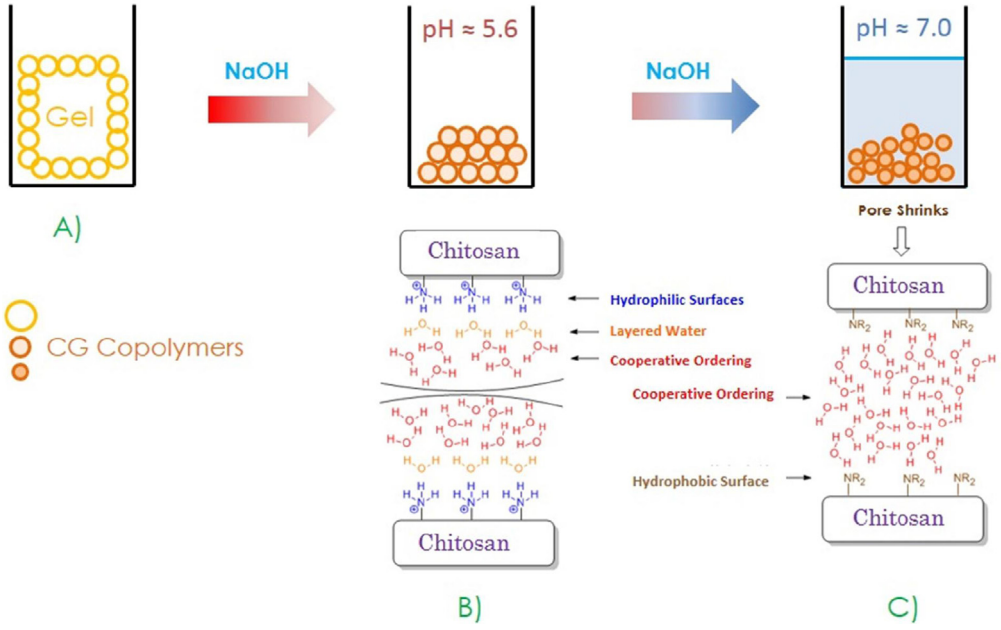

Fig. 2. The gel phase can be divided into several stages for the synthesis of the Chi-Glu copolymers: (a) aged gel for the CG copolymers; (b) after addition of 3–4 ml of NaOH and rigorous stirring with a spatula. The solution currently has a pH ≈ pK_a (chitosan) = 5.6 (Jin & Bai, 2002). Particles are swollen due to an opposing dipole caused by water. (c) Shrinkage of gel network and expulsion of water occurs. The recorded pH was 6.9.

lightest colour while CG-3 is the darkest in appearance. An exception to this trend occurs when the reaction conditions are changed according to temperature. The darkest copolymer is assigned to CG-2T since enal adducts are formed at higher temperatures. Therefore, the colours of the copolymers prepared at higher temperature are suggestive of the amount of enals and not necessarily the reagent ratios. The colour of the CG-1H copolymer was heterogeneous. The mechanism for the formation of Chi-Glu at basic pH conditions accelerates the polymerization of aldol on the surface of the copolymer since the reactions in the pore domains are considered slower due to the reduced intra-particle diffusion (Crini & Badot, 2008). The irregular polymerization explains the variable and heterogeneous appearance of CG-1H (*cf.* Fig. S1). If the surface of the CG-1 becomes less porous due to greater cross-linking at chitosan surface sites, the cross-linking of glutaraldehyde at the micropore domains is likely to be attenuated. Therefore, the amount of cross-linking within the interior of the particle is less than the surface and will have a lighter colour (Monteiro & Airoldi, 1999). Synthesis of CG-1 at higher pH conditions yielded a heterogeneous mixture of compounds with a denser copolymer phase. Copolymers with greater density are formed when sufficient water is removed from the pores in the product since the gel network collapses and the chitosan copolymer framework is more compact (Crini & Badot, 2008).

3.2. FT-IR spectroscopy

The FT-IR spectra of the various copolymers were characterized using FT-IR spectroscopy as shown in Fig. 4. The symbol "ν" denotes vibrational modes involved with the stretching of bonds while δ denotes the bending or deformation of bonds. Subscripts "as" denotes asymmetry while "s" denotes symmetrical vibrational modes. A detailed characterization of chitosan using FT-IR is complicated since many of the functional groups of both chitosan and the corresponding Chi-Glu copolymers contribute absorption bands with similar frequency. Consequently, this means that certain spectral regions for chitosan and the copolymers result from combinations of bands due to multiple functional groups.

The vibrational band at 2259 cm^{-1} is attributed to the presence of primary ammonium cations and result from several fundamental vibrational modes. Changes in the intensity of this combination band will indicate reactions involving the ammonium nitrogen centre. The presence of an amide group is assigned to the vibrational band at 1665 cm^{-1} [ν_{as}(C=O)]. The IR band at 1596 cm^{-1} corresponds to combined deformations of the primary amine groups [$\delta(NH_2)$], deformation of the primary ammonium cation, and an asymmetric stretching band for C—N in the amide [ν_{as}(C—N)], and the amide II. These results agree with previous results for chitosan (Kyzas, Kostiglou, & Lazaridis, 2008).

Chitosan can undergo multiple reactions with glutaraldehyde according to an amine-catalyzed aldol condensation, Michael addition or a Schiff base pathway depending on the reaction conditions (Kildeeva et al., 2009; Migneault, Dartiguenave, Bertrand, & Waldron, 2004). The cross-linking reaction employed herein involves reaction of glutaraldehyde with the amino groups of chitosan to form an imine cross-link. This cross-linking reaction for the various copolymers is supported by the FT-IR results according to the disappearance of the $\delta(NH_2)$ band at 1596 cm^{-1} and the formation of the imine band ν_{as}(C=N) at 1675–1680 cm^{-1}. The attenuation of the ammonium combination band at 2259 cm^{-1} and the $\delta_s(NH_2)$ band at 1596 cm^{-1} is attributed to deprotonation of the ammonium cation and cross-linking with glutaraldehyde (cf. Fig. 4). Additional evidence of a Schiff base adduct is supported by the new band at 1400 cm^{-1}. This vibrational band is analogous to the deformation of the C—H band observed for aldehydes; however, the signature is for a Schiff base adduct.

The occurrence of enal products derived from an aldol condensation is further supported by the presence of the ν_{as}(C=C) band at 1576 cm^{-1} as seen for the various copolymers. The intensity of the band at 1576 cm^{-1} relative to ν_{as}(C=N) provides a semi-quantitative estimate for the level of glutaraldehyde cross-linked with chitosan (Monteiro & Airoldi, 1999). According to synthetic conditions, CG-3 should have the highest glutaraldehyde content whereas CG-2 and CG-1 should be correspondingly less. The highest mass percentage of carbon is found in CG-3 according to the

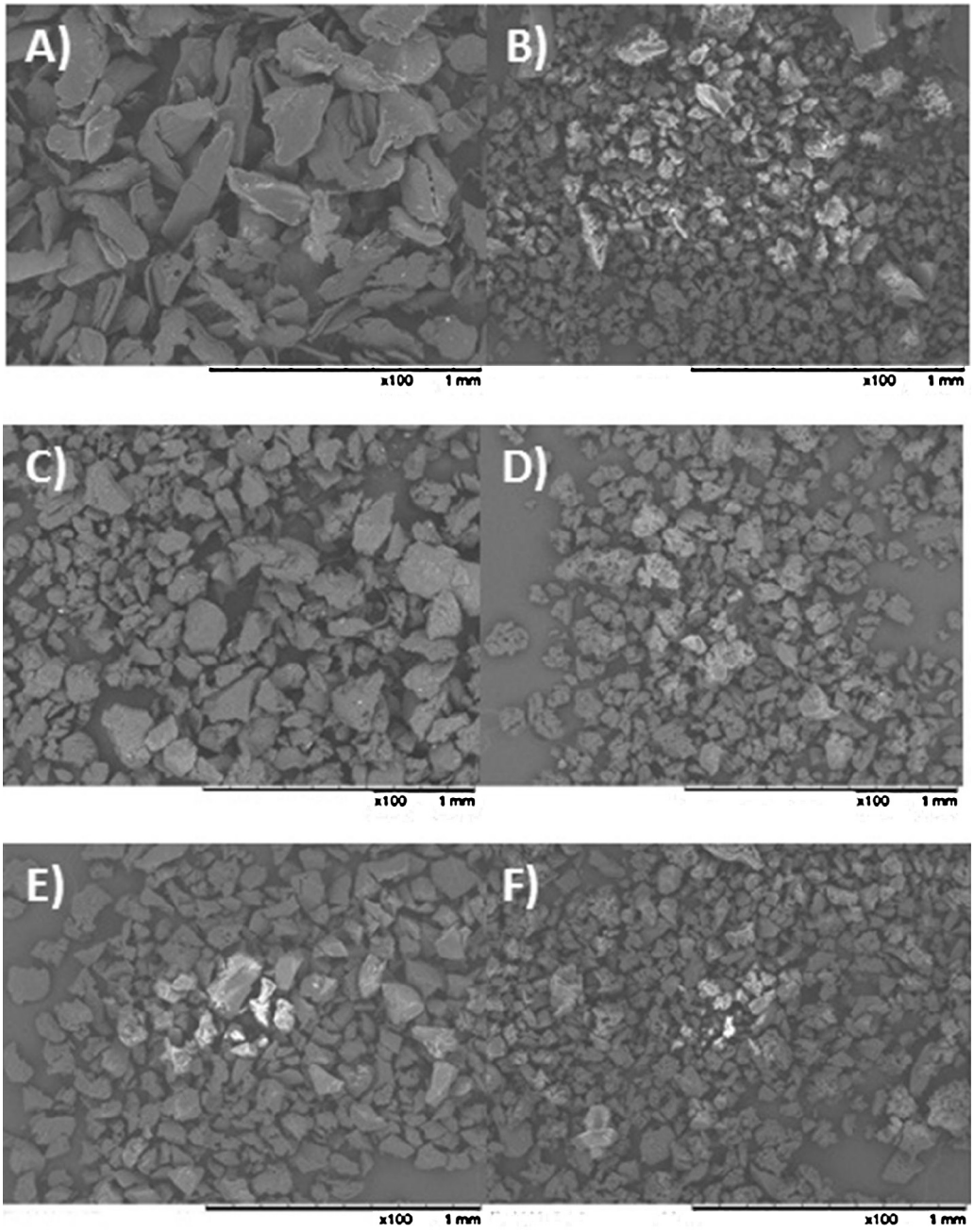

Fig. 3. SEM images with 100× magnification of the powdered copolymer products: (A) Chitosan; (B) CG-1; (C) CG-1H; (D) CG-2; (E) CG-2T; and (F) CG-3.

CHN data, and is anticipated to have the highest degree of cross-linking (Monteiro & Airoldi, 1999). The FT-IR results indicate that the CG-3 copolymer has the lowest level of cross-linking while the CHN analysis concludes the opposite. The apparent contradiction can be understood by the broad features of the vibrational band at 1576 cm^{-1}. This broad band is evidence that other vibrational modes contribute beside ν_{as}(C=N), such as the amide II and the ν_{as}(C=C) band.

3.3. TGA

TGA characterization of the polymers afford information about their relative thermal stability and relative cross-linker content (Wilson & Xue, 2013). A comparison of the thermal profile of pristine chitosan with polysaccharides such as guar gum (Gliko-Kabir, Penhasi, & Rubenstein, 1999), and cellulose (Basch & Lewin, 1973) reveals similar differential TGA profiles since each material possesses a similar thermal event at 300 °C. This is likely due to the scission of the glycosidic bonds between each chitosan monomer followed by pyrolytic weight loss.

In Fig. 5, the thermal event at 45–100 °C is attributed to loss of hydration from the copolymer. The aldol condensation of glutaraldehyde (Kildeeva et al., 2009) suggests that it may undergo self-polymerization, and this mechanism is supported by the broad combination band at 1576 cm^{-1}. Evidence of self-polymerization of glutaraldehyde is further shown by the higher temperature thermal event at 400 °C in Fig. 5. Different reports have suggested that glutaraldehyde may exist in a variety forms including glutaraldehyde homopolymers (Kildeeva et al., 2009; Migneault et al., 2004). Self-polymerization of glutaraldehyde is more likely as the glutaraldehyde content increases beyond the stoichiometric levels (i.e. >1:3 Glu-Chi) since there are three reaction sites per

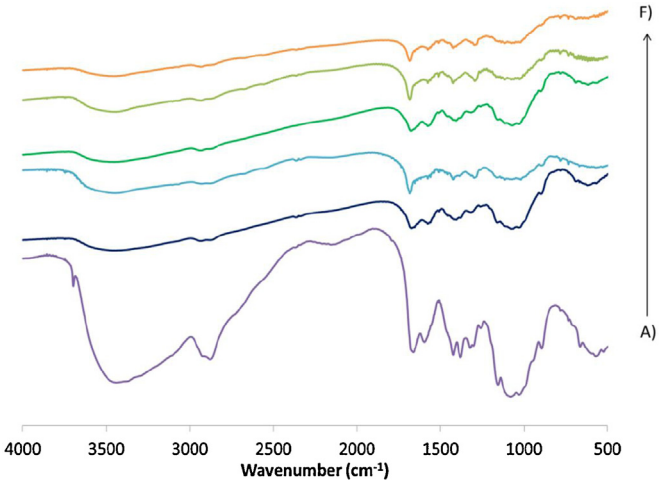

Fig. 4. FT-IR spectra of chitosan and Chi-Glu copolymers: (A) Chitosan; (B) CG-1; (C) CG-1H; (D) CG-2; (E) CG-2T; and (F) CG-3.

glucosamine monomer. Although two H-bond donor sites are lost due to cross-linking with one mole of glutaraldehyde, the branching of the framework structure increases. The cumulative van der Waals interactions from polymerization of glutaraldehyde may enhance the thermal stability of Chi-Glu copolymers. In the case of CG-2 and CG-3, the glutaraldehyde level exceeds the stoichiometric mole ratio of the amine group per monomer of chitosan. In Fig. 5, the thermal event at 400 °C provides evidence for self-polymerized glutaraldehyde within the copolymer framework. By comparison, the normal boiling point of monomeric glutaraldehyde is 188 °C (Wilson & Xue, 2013). The loss of cooperative H-bonding along the chitosan backbone in the case of the copolymers relates to changes in the available H-bond donor/acceptor sites due to cross-linking effects. Thus, the H-bond network is destabilized and a lower decomposition temperature occurs, as evidenced by the thermal event at ~240 °C, and appears lower than the transition for chitosan at ~280 °C. Therefore, the stability of the copolymer is strongly influenced by the level of cross-linking and the corresponding decrease in H-bonding between polymeric units of chitosan. Greater cross-linking and self-polymerization of glutaraldehyde occurs at elevated stoichiometric ratios of glutaraldehyde (i.e. >1:1 Chi:Glu) if one ignores reactions with the hydroxyl groups of chitosan or the self-polymerization of glutaraldehyde. The thermal

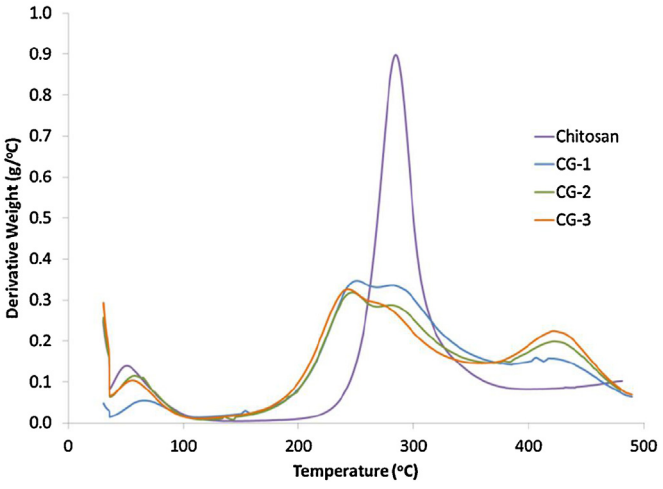

Fig. 5. The DTG results of Chi-Glu copolymers prepared at pH 7.0 and 298 K at various mole ratios. For CG-2T and CG-1H (see Figs. S1 and S2; Supporting Information).

stability of glutaraldehyde increases through cross-linking (or surface grafting with chitosan), while self-polymerization affords a more thermally stable polymer, in agreement with previous reports (Neto, Giacometti, Ferreira, Fonseca, & Pereira, 2005). TGA data for CG-1H and CG-2T are given in the supporting information (*cf.* Figs. S2 and S3).

3.4. CHN analysis

The CHN content can be used to derive an empirical formula. As the N content of chitosan remains constant throughout the reaction, it is possible to derive an experimental estimate of the mole ratio between glutaraldehyde and the monomer content of chitosan for the Chi-Glu copolymer materials. This calculation assumes the molecular weight and degree of deacetylation of chitosan are known. Chitosan is a polydisperse polymer with a distribution of molecular weights ranging from 40,000 to 190,000 kDa, according to the supplier. Size exclusion chromatography data reported elsewhere (Schatz, Viton, Delair, Pichot, & Domard, 2003) has shown that the polydispersity increases with an increasing degree of deacetylation. Since the degree of deacetylation is 75–85% (80% was used in foregoing calculation), it becomes possible to approximate the molecular weight range of chitosan using an average molecular weight value of 120,000 kDa (or g/mol). These assumptions are supported by the correspondence between the calculated and experiment CHN values for chitosan. The percent difference between the calculated and experimental C, H, and N values is 2.4%, 5.8%, and 2.3%, respectively. The results are reasonable in view of potential residual solvents and the estimated standard error (±5%) for CHN analysis.

The sole source of nitrogen is the amide and amine functional group at the C2 position of each glucosyl monomer unit of chitosan. Therefore, if the total number of chitosan monomers is known, the total N content may be calculated. The total number of monomers were calculated using the mole content of chitosan monomers and the degree of deacetylation. The resulting average number of individual monomer units is 714 where 596 contain amine groups and 118 monomers are acetylated. Using this result and the amount of water estimated from TGA enables estimates of the CHN content for chitosan and the Chi-Glu copolymers. The empirical formula of chitosan and the N content provides an estimate of the number of glutaraldehyde units bound to each chitosan monomer. These results are converted to Glu/NH_2 mole ratios in Table 4. The experimental Glu/NH_2 mole ratio assumes glutaraldehyde will react according to literature (Poon et al., 2014).

A comparison of calculated and experimental CHN results showed favourable agreement in most of the copolymers with an estimated error of 5–14%. The reasonable agreement for the glutaraldehyde content provides support for the validity of this method.

An interesting result is the observation of the limited cross-linking for CG-1H, a light orange powder. The elemental ratio is similar to Chi-Glu copolymers along with the colour and texture of similar copolymers reported elsewhere (Wilson & Xue, 2013). Secondly, the CHN results provide support that the glutaraldehyde undergoes self-polymerization because the total number of chitosan monomers with a free amine is 596. If two amines are consumed for every glutaraldehyde monomer reacted, then the total number of glutaraldehyde units that can undergo cross-linking via the amine group of chitosan is 298, where the Glu/NH_2 mole ratio is 0.5. Therefore, the CHN results should resemble CG-1H. Assuming that the experimental Glu/NH_2 mole ratio is correct, CG-1, CG-2, CG-2T, and CG-3 contain excess glutaraldehyde (cf. Table 1). According to the FT-IR results, there exists a small absorption band at 2259 cm^{-1} for the copolymers suggesting that free unbound ammonium ions are present. The occurrence of

Table 4
Experimental and theoretical CHN content of chitosan and its copolymers. The values were corrected for residual water content according to TGA estimates. The calculated number of glutaraldehyde and chitosan monomers are expressed as the Glu/NH_2 ratio.

Copolymer	Experimental			Experimental Glu/NH_2 ratio	Theoretical Glu/NH2 ratio	% Error
	%C	%H	%N			
Chitosan	41.6	7.46	7.67			
Chitosan[a](calculated)	42.6	7.05	7.85			
CG-1	44.4	6.97	5.44	(0.76 ± 0.13)	0.670	14
CG-1H	39.2	6.68	5.66	(0.42 ± 0.11)	0.670	38
CG-2	45.1	6.58	4.59	(1.23 ± 0.16)	1.17	5
CG-2T	45.8	6.70	4.57	(1.28 ± 0.16)	1.17	9
CG-3	46.9	6.71	4.20	(1.60 ± 0.18)	1.68	5

[a] The calculation assumes an average molecular weight of 120,000 kDa for chitosan with 80% deacetylation, and correction for residual water content from TGA results.

glutaraldehyde self-polymerization provides an understanding of the physicochemical properties of the copolymers which may contain excess glutaraldehyde. According to the CHN analysis, CG-3 has the highest glutaraldehyde content and possibly the highest level of self-polymerization. CG-2 and CG-1 have lower levels of glutaraldehyde, as evidenced by the TGA thermal event at 400 °C in Fig. 5. The physical appearance of CG-2T appears darker than CG-2, however, there are small differences in the cross-link density, according to the CHN results in Table 4. Therefore, there are limitations when using colour to estimate the cross-link density. The origin of the brown colouration is unknown but several explanations have been proposed that centre on the formation of a pyridinium ion adduct (Hardy, Hughes, & Rydon, 1979) or enal formation (Kildeeva et al., 2009).

3.5. Sorption of p-nitrophenol (PNP)

3.5.1. Effects of pH variation and glutaraldehyde content

Single-point sorption tests were carried out at a fixed concentration of PNP and constant adsorbent dosage at variable pH (*cf.* Fig. 6). Zeta-potential studies of Chi-Glu aerogels have demonstrated that the isoelectric point of these materials is close to pH 9.5 (Chang, Chen, & Jiao, 2008). Therefore, the surface charge of Chi-Glu copolymers adopts a positive zeta-potential for pH conditions (pH 4.6, 6.6, and 9.0) studied herein. The reported pK_a value for PNP was 7.15 (Kwon & Wilson, 2010) and although the total concentration of PNP remains constant, the speciation of the neutral and anionic forms of PNP will change as the pH varies. At pH 4.6, PNP is predominantly in its protonated form; whereas, ~58% is protonated at pH 6.6. At pH 9.0, PNP exists predominantly in its anion form.

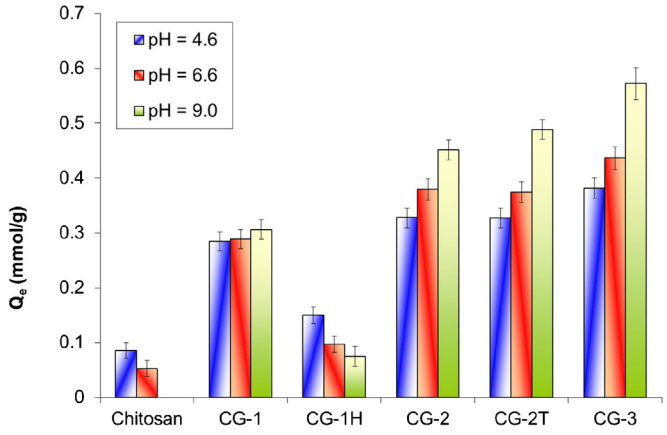

Fig. 6. Sorption of 10 mM PNP at various pH values. Note that the sorption capacity of chitosan with PNP at pH 9.0 was not measurable ($Q_e \sim 0$). Temperature of the PNP solution was 295 K and the pH was held constant with a 10 mM KH_2PO_4 (pH 4.6 and 6.6) and a 10 mM $NaHCO_3$ (pH 9.0) buffer.

According to single point isotherm results in Fig. 6, the sorption capacity increased from 0.285 mmol/g to 0.306 mmol/g for CG-1 as the pH increased from 4.6 to 9.0. A similar trend is observed for the other copolymers as the concentration of the PNP anion increased when the pH increased. The increasing sorptive uptake of PNP correlates with increasing cross-link level of the copolymer. The enhanced uptake of PNP occurs for a variety of reasons, increased pore structure of the framework sorption sites or a positive zeta-potential of the copolymer framework sites for anion binding. The occurrence of cross-linking of chitosan with glutaraldehyde renders the copolymer with increased positive zeta-potential, analogous to the positive zeta-potential of Chi-Glu aerogels up to pH 9.5 (Chang et al., 2008). In general, the sorption capacity increases as the cross-link density increases for the various copolymers. Cross-linking results in favourable changes of the textural properties of the copolymers relative to chitosan, in agreement with the results found by Crini and Badot, and by Wilson and Xue, but are contradicted by other studies (Chiou & Chuang, 2006; Pratt et al., 2013). Cross-linking of Chi-Glu materials is anticipated to change the surface chemistry and textural properties of chitosan, and the corresponding uptake of adsorbates that possess hydrophilic vs. hydrophobic character. To gain a further understanding of the effect of cross-linking, the sorptive uptake is plotted against the Glu/NH_2 ratios, as shown in Fig. 7. Pratt et al. (2013) studied a related Chi-Glu copolymer system but at much higher Glu/NH_2 ratios and those results are included for comparison. Fig. 7 shows a maximum in the sorptive uptake of PNP at a particular Glu/NH_2 ratio. Specifically, the

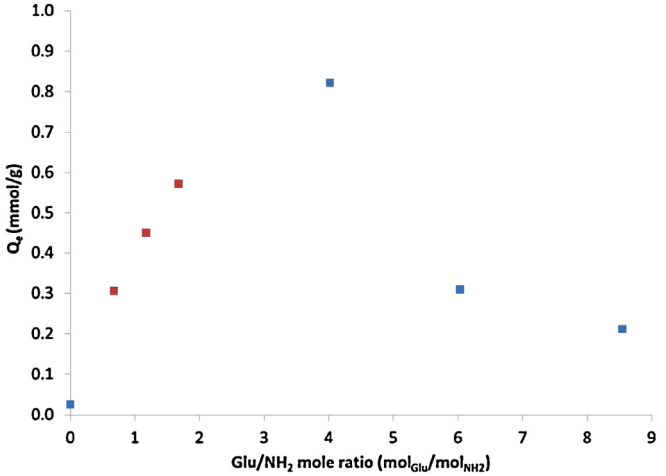

Fig. 7. Relative uptake of PNP at pH = 9.0 using chitosan and Chi-Glu copolymers at various experimental mole ratios. The red points correspond to the results obtained in this study; whereas, the blue points are data obtained from the literature (Pratt et al., 2013). CG-1 correlates to a 0.8 Glu/NH_2 ratio while CG-2 and CG-3 corresponds to Glu/NH_2 ratios of 1.2 and 1.6, respectively.

Table 5
Sorptive uptake of the copolymers at a fixed concentration (10 mM) of PNP for various pH conditions. The dosage of copolymer was fixed at 20 ± 1 mg.

Copolymers	Uptake at pH 4.6 (Q_e, mmol/g)	Uptake at pH 6.6 (Q_e, mmol/g)w	Uptake at pH 9.0 (Q_e, mmol/g)
Chitosan	0.085	0.052	ND*
CG-1	0.285	0.289	0.306
CG-1H	0.150	0.096	0.075
CG-2	0.327	0.378	0.451
CG-2T	0.327	0.374	0.488
CG-3	0.381	0.436	0.572

sorptive uptake increases when the cross-link density increases up to a Glu/NH_2 mole ratio of ~4 (CG-3) where a maxima is seen in Fig. 7. The trend coincides with reaction of the total available sites (i.e. —OH and —NH_2) of the chitosan monomer, along with some self-polymerization of glutaraldehyde. The degree of substitution agrees with the reduced steric effect of such linear polysaccharides relative to increased steric effects observed for related amylose-based urethane copolymers (Mohamed, Wilson, & Headley, 2011). The copolymers in this study contain enough glutaraldehyde to enhance sorption capacity as noted in a study by Kyzas et al. (2008). The relationship between the glutaraldehyde content of the copolymers reveals a synergistic dependence and this may relate to the formation of cross-links at amine and hydroxyl groups, along with some glutaraldehyde self-polymerization. The level of cross-linking employed herein does not reveal any noticeable steric effects since dye sorption is not attenuated significantly. However, excess glutaraldehyde may result in further cross-linking of the copolymer framework or self-polymerization of glutaraldehyde, and the resulting steric effect will decrease the sorption capacity.

3.5.2. Swelling properties: accessibility of sorption sites

In Table 5, the degree of swelling in water increases as the cross-link density increases, and differs from values reported in other studies (Chiou & Chuang, 2006; Pratt et al., 2013). According to the results in Table 6, there is a correlation between the level of swelling and an increase in the sorption capacity. The ratio of the increase in swelling (R_w) is provided in Table 6 which illustrates the difference between the copolymers and chitosan (*cf.* Eq. (3)). The ratio of the increase for the relative sorptive uptake (R_Q) is calculated similarly to the former using the sorptive uptake values and Eq. (4). The ratios for the swelling and the sorptive uptake for CG-2 and CG-2T are similar. In the case of the copolymers such as CG-1, CG-2, CG-2T, and CG-3, the relative accessibility to the sorption sites is an important factor in enhancing sorptive uptake, and illustrates the importance of textural properties for such materials. The relative accessibility of the sorption sites accounts for the appearance of a maximum in the sorption capacity observed in Fig. 7. At high levels of glutaraldehyde, the occurrence of self-polymerization or the formation of surface grafted glutaraldehyde may attenuate the accessibility of the active sorption sites. The latter is attributed to the hydrophilic character imparted by the glutaraldehyde units arising from the pendant carbonyl group as evidenced by the swelling behaviour of such materials (Wilson & Xue, 2013).

$$R_w = \frac{\%\text{swelling (copolymer)}}{\%\text{swelling (chitosan)}} \quad (3)$$

$$R_Q = \frac{Q_e\,\text{(copolymer)}}{Q_e\,\text{(chitosan)}} \quad (4)$$

3.5.3. Effect of solution temperature before gelation on sorption capacity

Another factor which affects the copolymer properties is the temperature conditions of the solution prior to gelation. There does not appear to be any relationship of this temperature with the sorptive uptake capacity of the materials, as evidenced for CG-2 (0.378 mmol/g) and CG-2T (0.374 mmol/g) at pH 6.6.

3.5.4. Effect of precipitation pH on sorption capacity

CG-1, CG-2, and CG-3 display greater sorption capacity relative to copolymer beads described in another independent study (Ngah & Fatinathan, 2006). Chitosan copolymers in the form of powders are known to have a higher sorption capacity and may have greater surface area (Kyzas et al., 2008). A question of interest is whether the sorption capacity of the beads is lower due to the surface chemistry or due to the difference in textural properties of beads vs. powders. An alkaline aqueous solution (pH 13.7) was previously reported for the cross-linking of glutaraldehyde with chitosan (Ngah & Fatinathan, 2006). These conditions were adopted for the synthesis for CG-1H where the Chi-Glu gel was precipitated out and the supernatant aqueous phase had a final pH at 12.8. Fig. 6 compares the sorptive uptake against pH which is markedly different for CG-1 and CG-1H. Although the sorptive uptake of CG-1 with PNP increases as the pH increases, the sorptive properties of CG-1H resemble those for chitosan and decrease with increasing pH. CG-1H undergoes more swelling than CG-1, and the reduced accessibility to the sorption sites does not account for the reduced sorptive uptake. The zeta-potential of such materials prepared at alkaline conditions may be attenuated but steric effects may occur where water can access the pores of the copolymer but PNP may be restricted. Attenuated sorption capacities in the case of Chi-Glu beads may be related to the reaction conditions which affect the density and pore structure of the copolymer material. Neutral pH during the precipitation step enhances the sorption capacity of the copolymers relative to chitosan. Excess base in the supernatant solution during precipitation causes a lowering of the sorption capacity. This is in agreement with differences in the copolymer zeta-potential for such reaction conditions.

Table 6
Swelling and adsorptive properties of adsorbent materials in aqueous solution at pH 6.6.

Sorbent material	Swelling (×10^3%)	Swelling Ratio (R_w)[a] in water	Relative Sorption (R_Q)[b] at pH 6.6
Chitosan	0.238	NA	NA
CG-1	0.770	3.24	5.51
CG-1H	0.901	3.79	1.87
CG-2	1.77	7.43	7.23
CG-2T	1.80	7.60	7.14
CG-3	3.11	13.1	8.33

[a] R_w is defined by Eq. (3).
[b] R_Q is defined by Eq. (4).

4. Conclusions

Chitosan and its copolymers were investigated at variable reaction conditions such as pH conditions during workup, gelation temperatures, and relative cross-linking ratios. This study examines the relationship between the sorption properties of the various sorbent materials with *p*-nitrophenol. Temperature conditions affect the physical appearance of the copolymers but there is no overall effect on the overall sorption capacity. The pH of the solution during precipitation and the cross-link ratio has a greater influence on the sorption capacity of the copolymers. Alkaline pH conditions can decrease the copolymer sorption capacity by a factor of 2–3 for copolymers with similar cross-link ratios. Increasing the cross-link ratio can initially increase the sorption capacity but a maximum occurs at the 4:1 Glu/NH_2 ratio. Higher glutaraldehyde content beyond the optimal ratio will result in attenuated sorption capacity due to potential changes in surface chemistry and inaccessibility of the sorption sites.

Acknowledgement

The authors gratefully acknowledge the University of Saskatchewan and Environment Canada for supporting this research.

Appendix A. Supplementary data

Supplementary data associated with this article can be found, in the online version, at http://dx.doi.org/10.1016/j.carbpol.2014.02.086.

References

Basch, A., & Lewin, M. (1973). The influence of fine structure on the pyrolysis of cellulose. I. Vacuum pyrolysis. *Journal of Polymer Science: Part A*, *11*, 3071–3093.
Bodnar, M., Hartmann, J., & Borbely, J. (2006). Synthesis and study of cross-linked chitosan-*N*-poly(ethylene glycol) nanoparticles. *Biomacromolecules*, *7*, 3030–3036.
Bodnar, M., Hartmann, J. F., & Borbely, J. (2005). Preparation and characterization of chitosan-based nanoparticles. *Biomacromolecules*, *6*, 2521–2527.
Brinker, C. J., & Scherer, G. (1990). *Sol–gel science: The physics and chemistry of sol–gel processing*. London: Academic Press.
Bruck, W., Slater, J., & Carney, B. (2010). Chitin and chitosan from marine organisms. In K. Se Kwon (Ed.), *Chitin, chitosan, oligosaccharides, and their derivatives: Biological activities and applications* (pp. 11–24). Boca Raton, FL: Taylor & Francis.
Chang, X., Chen, D., & Jiao, X. (2008). Chitosan-based aerogels with high adsorption performance. *Journal of Physical Chemistry B*, *112*, 7721–7725.
Chen, X., Zheng, L., Wang, Z., Lee, C., & Park, H. (2002). Molecular affinity and permeability of different molecular weight chitosan membranes. *Journal of Agricultural and Food Chemistry*, *50*, 5915–5918.
Chiou, M., & Chuang, G. (2006). Competitive adsorption of dye metanil yellow and RB15 in acid solutions on chemically cross-linked chitosan beads. *Chemosphere*, *62*, 731–740.
Chiou, M. S., & Li, H. Y. (2003). Adsorption behavior of reactive dye in aqueous solution on chemical cross-linked chitosan beads. *Chemosphere*, *50*, 1095–1105.
Crini, G., & Badot, P. M. (2008). Application of chitosan, a natural aminopolysaccharide, for dye removal from aqueous solutions by adsorption processes using batch studies: A review of recent literature. *Progress in Polymer Science*, *33*, 399–447.
Ghosh, B., & Urban, M. (2009). Self-repairing oxetane-substituted chitosan polyurethane networks. *Science*, *323*, 1458–1460.
Gliko-Kabir, I., Penhasi, A., & Rubinstein, A. (1999). Characterization of crosslinked guar by thermal analysis. *Carbohydrate Research*, *316*, 6–13.
Hardy, P. M., Hughes, G. J., & Rydon, H. N. (1979). The nature of the cross-linking of proteins and glutaraldehyde. Part 2. The formation of quaternary pyridinium compounds by the action of on proteins and the identification of a 3-(2-piperidyl)pyridinium derivative, anabilysine, as a cross-linking entity. *Journal of the Chemical Society, Perkin Transactions*, *1*, 2282–2288.
Henry, L., Puspitasari-Nienaber, N., Jarén-Galán, M., van Breeman, R., Catignani, G., & Schwartz, S. (2000). Effects of ozone and oxygen on the degradation of carotenoids in an aqueous model system. *Journal of Agricultural and Food Chemistry*, *48*, 5008–5013.
Jafarinejad, S., Gilani, K., Moazeni, E., Ghazi-Khansari, M., Najafabadi, A., & Mohajel, N. (2012). Development of chitosan-based nanoparticles for pulmonary delivery of itraconazole as dry powder formulation. *Powder Technology*, *222*, 65–70.
Jin, L., & Bai, R. (2002). Mechanisms of lead adsorption on chitosan/PVA hydrogel beads. *Langmuir*, *18*, 9765–9770.
Kildeeva, N., Perminov, P., Vladimirov, L., Novikov, V., & Mikhailov, S. (2009). *Russian Journal of Bioorganic Chemistry*, *35*, 360–369.
Kwon, J. H., & Wilson, L. D. (2010). Activated carbon surface-modified with β-cyclodextrin – Part II. Sorption properties. *Journal of Environmental Science and Health, Part A*, *45*(13), 1793–1803.
Kyzas, G. Z., Bikiaris, D. N., & Lazaridis, N. K. (2008). Low-Swelling Chitosan Derivatives as Biosorbents for Basic Dyes. *Langmuir*, *24*, 4791–4799.
Kyzas, G. Z., Kostoglou, M., & Lazaridis, N. K. (2010). Relating Interactions of Dye Molecules with Chitosan to Adsorption Kinetic Data. *Langmuir*, *26*, 9617–9626.
Lu, P., Ma, Y., Yu, R., Yue, H., Dezhi, N., Wei, W., et al. (2012). Targeted delivery of insoluble cargo (Paclitaxel) by PEGylated chitosan nanoparticles grafted with Arg-Gly-Asp (RGD). *Molecular Pharmaceutics*, *9*, 1736–1747.
Ma, G., Qian, B., Yang, J., Hu, C., & Nie, J. (2010). Synthesis and properties of photosensitive chitosan derivatives. *International Journal of Biological Macromolecules*, *46*, 558–561.
Mansri, A., Memou, C. H., & Benabadji, K. I. (2013). Synthesis and pNP interactions of a new copolymer poly(4-vinylpyridine-G-(6-o-monotosyl-6-desoxy-β-cyclodextrin)). *Research on Chemical Intermediates*, http://dx.doi.org/10.1007/s11164-013-1307-9
Migneault, I., Dartiguenave, C., Bertrand, M. J., & Waldron, K. C. (2004). Glutaraldehyde: Behavior in aqueous solution, reaction with proteins, and application to enzyme crosslinking. *BioTechniques*, *37*, 790–802.
Mohamed, M. H., Wilson, L. D., & Headley, J. V. (2011). Design and characterization of novel β-cyclodextrin based copolymer materials. *Carbohydrate Research*, *346*, 219–229.
Monteiro, O. A. C., Jr., & Airoldi, C. (1999). Some studies of crosslinking chitosan-glutaraldehyde interaction in a homogeneous system. *International Journal of Biological Macromolecules*, *26*, 119–126.
Muzzarelli, R. A. A. (1977). *Chitin*. Toronto, ON: Pergamon Press.
Neto, C. G. T., Giacometti, J. A., Ferreira, F. C., Fonseca, J. L. C., & Pereira, M. R. (2005). Thermal analysis of chitosan based networks. *Carbohydrate Polymer*, *62*, 97–103.
Ngah, W. S. W., & Fatinathan, S. (2006). Chitosan flakes and chitosan-GLA beads for adsorption of *p*-nitrophenol in aqueous solution. *Colloids and Surfaces A: Physicochemical Engineering Aspects*, *277*, 214–222.
Piron, E., Accominotti, M., & Domard, A. (1997). Interaction between chitosan and uranyl ions. Role of physical and physicochemical parameters on the kinetics of sorption. *Langmuir*, *13*, 1653–1658.
Poon, L. (2103). M.Sc. Thesis, University of Saskatchewan, Saskatoon, SK.
Poon, L., Younus, S., & Wilson, L. D. (2014). Adsorption study of an organo-arsenical with chitosan-based sorbents. *Journal of Colloid and Interface Science*, *420*, 136–144.
Pratt, D. Y., Wilson, L. D., & Kozinski, J. A. (2013). Preparation and sorption studies of glutaraldehyde cross-linked chitosan copolymers. *Journal of Colloid and Interface Science*, *395*, 205–211.
Schatz, C., Viton, C., Delair, T., Pichot, C., & Domard, A. (2003). Typical physicochemical behaviors of chitosan in aqueous solution. *Biomacromolecules*, *4*, 641–648.
Shu, X. Z., & Zhu, K. J. (2002). The influence of multivalent phosphate structure on the properties of ionically cross-linked chitosan films for controlled drug release. *European Journal of Pharmaceutics and Biopharmaceutics*, *54*, 235–243.
Wilson, L. D., & Xue, C. (2013). Macromolecular sorbent materials for urea capture. *Journal of Applied Polymer Science*, *128*, 667–675.
Wilson, L. D., Mohamed, M. H., & Headley, J. V. (2011). Surface area and pore structure properties of β-cyclodextrin-urethane copolymer materials. *Journal of Colloid and Interface Science*, *357*, 215–222.
Xu, D., Hein, S., Loo, S., & Wang, K. (2008). The fixed-bed study of dye removal on chitosan beads at high pH. *Industrial & Engineering Chemistry Research*, *47*, 8796–8800.
Youn, D., No, H., & Prinyawiwatkul, W. (2007). Physical characteristics of decolorized chitosan as affected by sun drying during chitosan preparation. *Carbohydrate Polymer*, *69*, 707–712.